International Journal of Emerging Technology and Advanced Engineering
Website: www.ijetae.com (ISSN 2250-2459, ISO 9001:2008 Certified Journal, Volume 7, Issue 8, August 2017)

Design of Single Neuron Adaptive PID Controller for Levitation Control of Hybrid Bearingless Switched Reluctance Motor

Polamraju. V. S. Sobhan[1], G. V. Nagesh Kumar[2], P. V. Ramana Rao[3]
[1]*Dept. of EEE, VFSTR University, Guntur, India*
[2]*Dept. of EEE, VIIT, Visakhapatnam, India*
[3]*Dept. of EEE, Acharya Nagarjuna University, Guntur, India*

***Abstract*— The hybrid pole type bearingless switched reluctance motor (BSRM) is a nonlinear multi-variable system with extensive variety of uses in space science, PV cell, high-speed turbo machineries, flywheel energy storage, aerospace, and so on. In the BSRM, the amount and orientation of the levitation force depends on the rotor eccentricity, which causes the unstable rotor levitation and speed ripples during the motor operation. A controller is essential to stabilize the rotor, to reduce vibration and to track the desired speed, and the conventional PID controller is not suitable since adjustment of its parameters is not possible under different operating conditions. This paper presents an intelligent control strategy blending the features of ANN and PID controller, which can adjust the controller parameters by adjusting weights of neuron. The design of Single Neuron Adaptive PID (SNAPID) controller is carried out using Matlab/Simulink and the results have shown the effectiveness in reducing the torque and suspension force ripples under standstill and loaded conditions.**

***Keywords*—BSRM, levitation control, PID Controller, Single Neuron, Torque control.**

I. Introduction

The motors used in extreme industrial environments such as radioactive, vacuum, pharmaceutical, biochemical, etc. needs to have an ultrahigh cleanness with lubricant and pollution free feature in addition to low friction losses, small size, lightweight and low maintenance [1-2]. The mechanical bearings used in conventional motors requires frequent lubrication and maintenance are not suitable for these applications and the bearingless motors (BLMs) are becoming natural choice because of their advantageous features such as no-wear, no abrasion, compact size and high speed for these applications[3-6]. A bearingless motor integrates the motoring function with noncontact magnetic levitation of rotor within the same stator frame [7]. The BLMs, consists two sorts of windings on stator, which have distinctive pole numbers, for the torque and rotor levitation.

The flux distribution in the air gap is irregular due to excitation of the levitation winding and the regulation of rotor eccentricity is achieved by levitation force. The magnetic levitation force and torque can be created in a same unit and their control is carried out with less number of power electronic converters, controllers, and connection wires when contrasted with a motor having magnetic bearings.

The bearingless switched reluctance motor (BSRM) has been given careful consideration because of its propelled attributes of simple structure, dependable operation, high effectiveness and creation of extraordinary levitation force [8-10]. In the BSRM, the rotor levitation is the outcome of the collaborations between the torque windings flux and the levitation windings flux, which decides the solid dependency between torque and levitation control. Thus, the independent control of the torque and levitation force is essential for smooth the operation of a BSRM [11].

The design of suitable control system for the levitation of BSRM in view of decoupling is critical for true operation of a BSRM. Along these lines, it is important to consider on the control techniques for the levitation of BSRM [12-13].. The parameters of conventional PID controllers used to control the rotor levitation, have the fixed values when the motor operating in a specific state. Whenever the motor parameters or state changes, the performance will be influenced, and the dynamic and steady state accuracy cannot be guaranteed. Similarly, it is exceptionally troublesome for this control scheme to get an adequately high-performance control to the BSRM system, which is a, nonlinear- multivariable and strongly coupling system with time-dependent parameters.

This paper aims to develop a control strategy blending the features of robustness, better dynamic response and less computation time of ANN and set point tracking precision of PID controller [14-15]. The levitation and torque control system of BSRM with power converter is designed in MATLAB/SIMULINK.

International Journal of Emerging Technology and Advanced Engineering
Website: www.ijetae.com (ISSN 2250-2459, ISO 9001:2008 Certified Journal, Volume 7, Issue 8, August 2017)

The results demonstrate that the SNAPID controller has enhanced the exactness of levitation control, speed tracking with less ripples of BSRM compared with conventional PID controller.

II. HYBRID POLE 12/14 BSRM

The stator pole and winding structure of 12/14 BSRM shown in Fig.1. The 12 poles of stator consists two distinct windings, 8 for torque generation and 4 for levitation, this structure minimizes the dependency of levitation force on torque generation unlike in regular SRM. The torque production is due to formation of two phases A and B each phase with 4 stator poles connected in series P_{A1} to P_{A4} and P_{B1} to P_{B4} and torque is regulated by the currents i_A and i_B same as in conventional SRM. The rotor levitation and eccentric control in all the four directions of x-y plane is achieved by controlling the currents i_{xp} , i_{xn} , i_{yp} and i_{yn} independently, flowing in the four poles P_{xp}, P_{xn}, P_{yp} and P_{yn}.

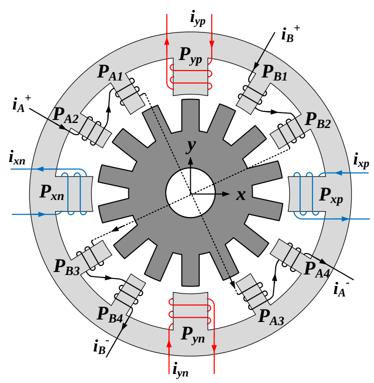

Figure 1 Hybrid BSRM pole structure

Fig. 2 demonstrates the dependency of torque and levitation force of BSRM. The viable region of torque is from position 1 to 3 and accessible levitation force starts from position 2 to 4. From positions 2 to 3, the overlapping of torque and levitation force occurs and this region is highly suitable for the motor to generate sufficient torque and levitation force in the meantime. This region is extremely thin due to the fundamental nature of torque and levitation force generation. So the working point must be chosen to trade off amongst torque and levitation force when utilizing the regular structure and full utilization of torque and levitation force regions is not possible. Hence to acquire enough levitation the increase in current in essential and dwell angle ought to be shifted towards aligned position.

This leads in increased copper loss and thermal issues because of the increase in current value to get higher torque or levitation force. But with the common winding current the simultaneous generation of torque or levitation force happens and are non linearly depends on current and position. In this manner, it is extremely hard to decouple the torque from levitation force.

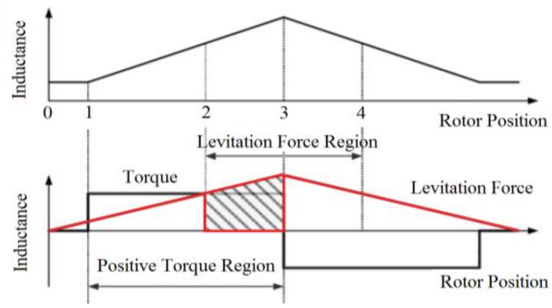

Figure 2 Inductance profile of SRM

The eccentric error due to dislodging of the rotor of BSRM because of the non-presence of mechanical bearings. The unbalanced force on the rotor which is oriented towards fourth quadrant of x-y plane is shown in Fig.3. To pull the rotor back to center the required counter levitation force F must be towards second quadrant and is the resultant of F_x and F_y , the produced levitation forces in negative x and positive y directions.

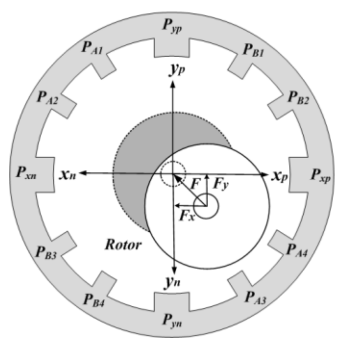

Figure 3 Eccentricity effect of the air-gap displacement

III. SINGLE NEURON ADAPTIVE PID CONTROLLER

It is hard to acquire the correct model of complex non-linear, uncertain BSRM and its parameters fluctuate with the working conditions so it is necessary to adjust the PID control parameters online as per the dynamic data of the system. The single neuron with variable weights has the benefit of self adaptive and is utilized to adjust the PID parameters online. The structure of SNAPID controller is shown in Fig.4.

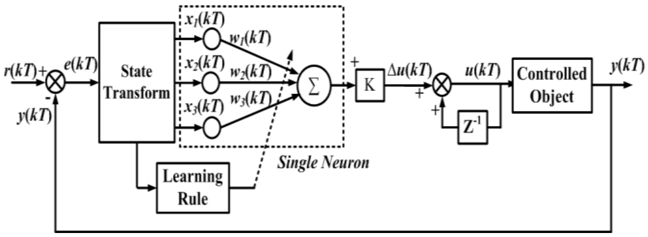

Figure 4 Proposed SNAPID control system

The deviation of actual output $y(kT)$ from the reference input $r(kT)$ is the error $e(kT)$ and is transformed into three input variables of the neuron as given in (1)

$$\begin{aligned} x_1(kT) &= e(kT) \\ x_2(kT) &= e(kT) - e((k-1)T) \\ x_3(kT) &= e(kT) - 2e((k-1)T) + e((k-2)T) \end{aligned} \quad (1)$$

The output of the neuron is expressed as

$$u(kT) = u((k-1)T) + K\sum_{i=1}^{3} x_i(kT)\, w_{Ni}(kT) \quad (2)$$

$$w_{Ni}(kT) = \frac{w_i(kT)}{\sum_{i=1}^{3} |w_i(kT)|} \quad (3)$$

Where $u(kT)$ is the output, $w_{Ni}(kT)$ is the normalized weight and K is the positive scale factor of the neuron. The self-learning of the neuron is implemented by adjusting weights $w_i(kT)$, i=1,2,3 using supervised Hebb's learning and the updated weights are given by equation.

$$\begin{aligned} w_1(kT) &= w_1((k-1)T) + \eta_I K\, \rho(kT)\, u(kT)\, x_1(kT) \\ w_2(kT) &= w_2((k-1)T) + \eta_P K\, \rho(kT)\, u(kT)\, x_2(kT) \\ w_3(kT) &= w_3((k-1)T) + \eta_D K\, \rho(kT)\, u(kT)\, x_3(kT) \end{aligned} \quad (4)$$

Where $\rho(kT)$=$e(kT)$ is the output error and η_I ,η_P and η_D are learning rates of integral, proportional and differential parts respectively, which are used to modulate the different weights $w_{Ni}(kT)$.

The rules for determining the adjustable parameters K, η_I, η_P and η_D are

1. If the step response contains large overshoot and oscillations then K should be reduced , if the response is without overshoot and large rise time then K should be increased and in both conditions the three learning rates are unchanged
2. If the response contains frequent sine attenuation, then reduction in η_P is required keeping the other parameters unchanged.
3. If the speed of the response is fast and contains large overshoot, then reduction in η_I is required while keeping the other parameters unchanged.
4. If the speed of the response is slow, η_I is required to increase, and if contains large overshoot corresponding increase in η_P is required while keeping the other parameters unchanged.
5. The initial value of η_D is to be small and the adjustment should be gradual.

IV. Simulation And Results

The Matlab/Simulink model of the BSRM as in shown in Fig.5, consists of four parts, the first two parts are for suspension control and speed control, the third part is the model of BSRM drive and the final part is speed sensing and feedback. The suspension control is for positioning the rotor in the stator eccentric in both x- and y-axis directions.

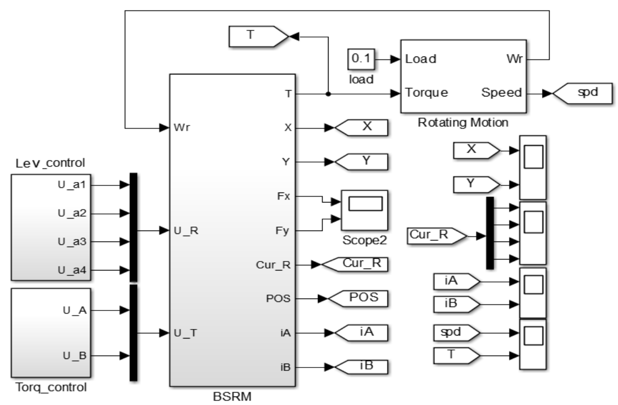

Figure 5 The SNAPID controlled BSRM system Simulink model

The suspension control part of the BSRM system with SNAPID Controller is shown in Fig. 6. The rotor position is controlled using the error between the reference (eccentric center of stator) and actual positions x- and y-axis directions. The two Controllers output forces commands ($F_x^*$and F_y^*), are converted into levitation winding reference currents ($i_x^*$and i_y^*), which are compared with the BSRM actual currents using current signal block to derive current signals x_2, x_4, y_1 and y_3 . The current selection block calculates the currents in x and y axis suspension windings using on the reference forces $F_x^*$and F_y^*, from two controllers and x_2, x_4, y_1 and y_3. These currents, actual winding currents, actual motor forces, reference voltages are calculated and applied to four windings of suspension poles (electromagnets).

International Journal of Emerging Technology and Advanced Engineering
Website: www.ijetae.com (ISSN 2250-2459, ISO 9001:2008 Certified Journal, Volume 7, Issue 8, August 2017)

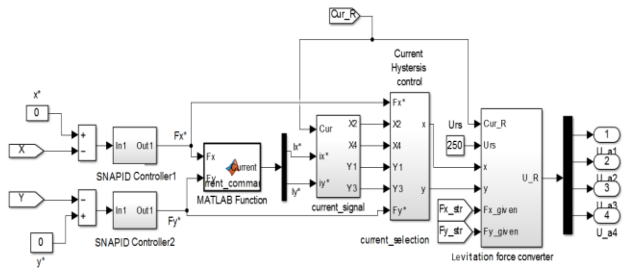

Figure 6 Simulink model of the suspension control part

The torque and motor speed control on load is implemented using torque control block shown in Fig.7. The input to the controller is the difference between the set value and actual motor speed and produces main axis reference current as output. The controller output is compared with *A* and *B* phase winding currents and the errors are fed to the hysteresis controller which is a relay block, that allows only a band of current signals within the scope and produces PWM pulses for each phase. The torque converter produces PWM pulses G_1 and G_2 for the asymmetrical inverter to drive the motor with the inputs motor main windings, rotor position, stator voltage and a PWM pulse outputs from the hysteresis controller in *A* and *B* phases.

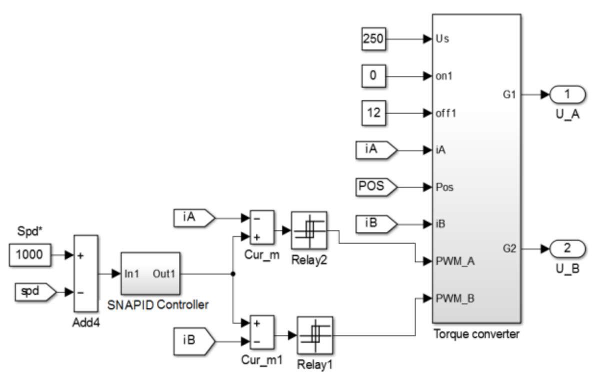

Figure 7 The Simulink model of the torque control part

The displacement of rotor in two directions (*x* and *y*) under no load condition is shown in Fig.8 and it can be observed that the rotor initial location is 120 µm in the direction of both the positive *x* and negative *y* axis.

With SNAPID controller, the rotor settles at center of the stator rapidly within 0.02 sec with no vibration, whereas with the conventional PID controller the rotor vibrates more in the *x*-direction than in the *y*-direction and stays at centre with ceaseless vibration.

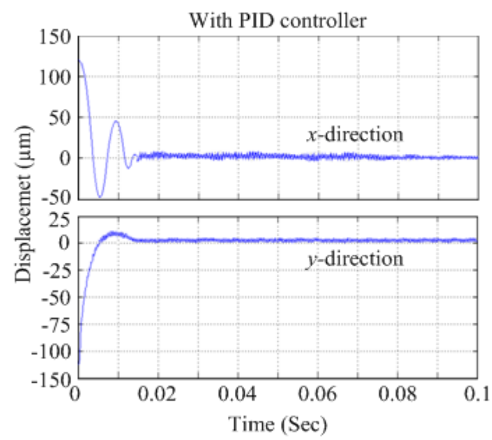

(a)

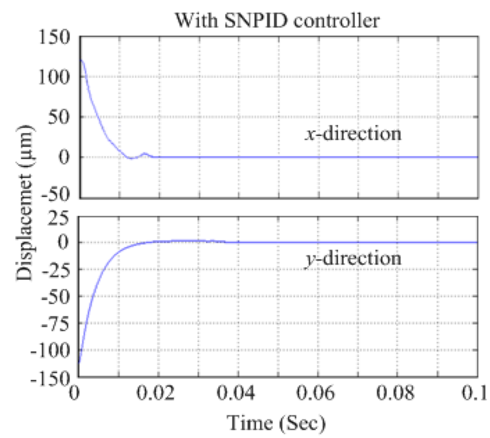

(b)

Figure 8 Rotor displacements with PID and SNAPID controllers

The force commands generated by both controllers are shown in Fig.9.The proposed two SNAPID controllers in the levitation control system generates high forces initially to bring the rotor to the centre and after that maintains constant value when compared to conventional PID controllers. The ripples in the force commands are eliminated by the single neuron.

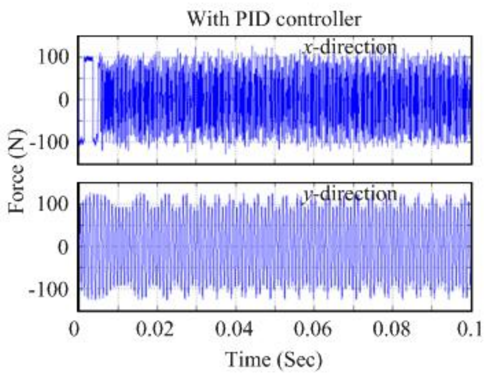

(a)

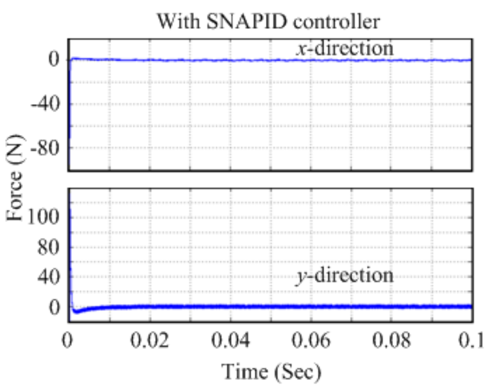

(b)

Figure 9 Generated resultant forces by PID and SNAPID controllers

Fig.10 shows the simulation results of speed and electromagnetic torque generated when the reference speed is 3000 rpm. From the fig, it can be observed that with the proposed controller smooth speed tracking is achieved with less settling time than with conventional controller and correspondingly the ripples in generated torque also minimized.

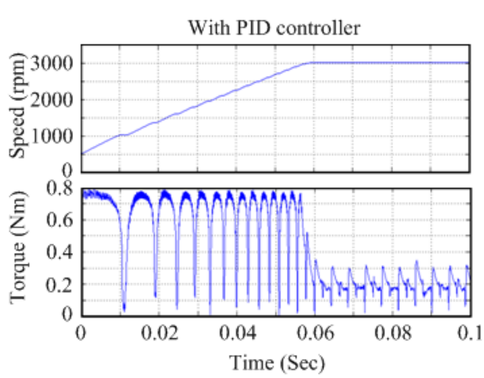

(a)

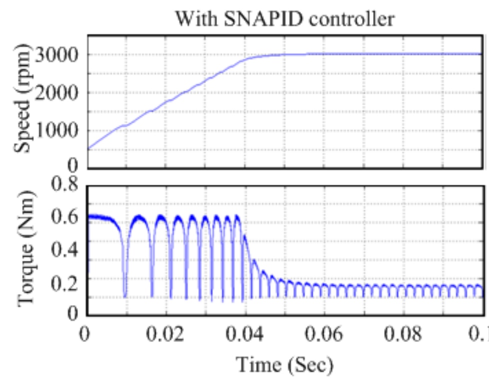

(b)

Figure 10 Speed and Torque generated with PID and SNAPID controllers

The currents drawn by two phases A and B when the rotor is tracking the set speed are shown in Fig.11, and it can be observed that the magnitude of currents reduces with the proposed controller

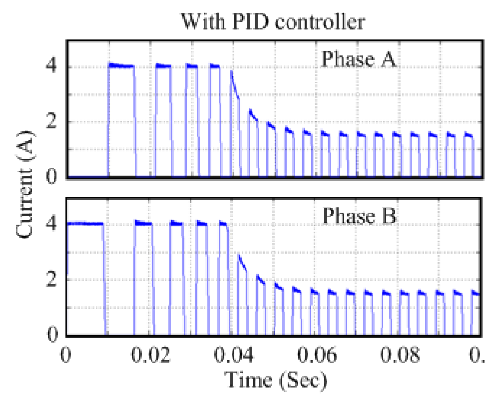

(a)

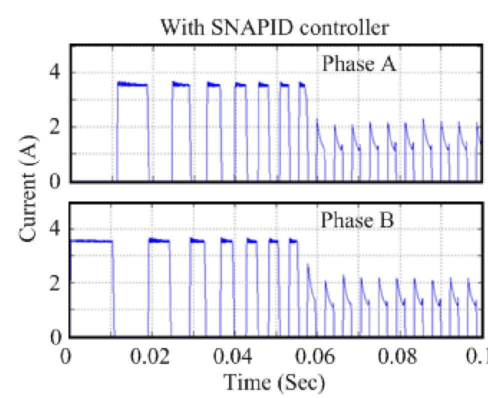

(b)

Figure 11 Currents in two phases with PID and SNAPID controllers

V. CONCLUSION

The hybrid pole structure of Bearingless SRM makes possible the control of rotor levitation and torque independently even in the presence of profound nonlinearities and uncertainties. This paper focuses on a hybrid control scheme using single neural system for tuning the PID gains for improving the levitation performance, reducing rotor vibrations and set-point speed tracking. Two SNAPID levitation controllers (*x* and *y* directions) and one SNAPID speed controller for BSRM are designed independently and simulated using MATLAB/Simulink. The online adjustment of PID gains can be achieved by single neuron with three inputs based on unsupervised Hebb algorithm. The result shows the effectiveness of the proposed control algorithm over conventional PID in terms of simple structure, improved levitation performance and stronger robustness in rotor vibration suppression.

REFERENCES

[1] R. Bosch, “Development of a bearingless electric motor,” in Proc. ICEM,Pisa, Italy, 1988, pp. 373–375.

[2] J. Bichsel, “The bearingless electrical machine,” in Proc. Int. Symp. Magn. Suspension Technol., Hampton, VA, USA, pp. 561–573, 1991.

[3] J. X. Shen, K. J. Tseng, D. M. Vilathgamuwa, and W. K. Chan, “A novel compact PMSM with magnetic bearing for artificial heart application,” IEEE Trans. Ind. Appl., vol. 36, no. 4, pp. 1061–1068, Jul./Aug. 2000.

[4] M. Ooshima, C. Takeuchi, “Magnetic suspension performance of a bearingless brushless DC motor for small liquid pumps,” IEEE Trans. on Industry Applications, vol. 47, no. 1, pp. 72-78, January 2011.

[5] Y. Okada, N. Yamashiro, K. Ohmori, “Mixed flow artificial heart pump with axial self-bearing motor,” IEEE/ASME Trans. on Mechatronics, vol. 10, no. 6, pp. 658-665, December 2005.

[6] J. X. Shen, K. J. Tseng, D. M. Vilathgamuwa, and W. K. Chan, “A novel compact PMSM with magnetic bearing for artificial heart application,” IEEE Trans. Ind. Appl., vol. 36, no. 4, pp. 1061–1068, Jul./Aug. 2000.

[7] L. Hertel, W. Hofmann, “Basic approach for the design of bearingless motors,” Proc. of the 7th Int. Sym. on Magnetic Bearings, Aug. 2000.

[8] S. Ayari, M. Besbes, M. Lecrivain, and M. Gabsi, “Effects of the airgap eccentricity on the SRM vibrations,” in Proc. Int. Conf. Elect. Mach.Drives, pp. 138–140, 1999.

[9] D.H.Lee and J.W. Ahn, “Design and analysis of hybrid stator bearingless SRM,” J. Elect. Eng. Technol., vol. 6, no. 1, pp. 94–103, 2011.

[10] C. R. Morrison, M. W. Siebert, and E. J. Ho, “Electromagnetic forces in a hybrid magnetic-bearing switched-reluctance motor,” IEEE Trans. Magn., vol. 44, no. 12, pp. 4626–4638, Dec. 2008.

[11] L. Chen and W. Hofman, “Analytically computing winding currents to generate torque and levitation force of a new bearingless switched reluctance motor,” in Proc. 12th Int. Power Electron. Motion Control Conf., Portoroz Slovenia, 2006, pp. 1058–1063

[12] L. Chen and W. Hofmann, “Performance characteristics of one novel switched reluctance bearingless motor drive,” in Proc. PCC, Nagoya, Japan, 2007, pp. 608–613.

[13] Zhenyao Xu, Dong-Hee Lee and Jin-Woo Ahn, “Comparative Analysis of Bearingless Switched Reluctance Motors With Decoupled Suspending Force Control,” IEEE Transactions on Industry Applications, vol. 51, no. 1, pp 733-743, 2015.

[14] Zhang Yinga, LI Penga and WU Wen-jiangb, “Single Neuron PID Sliding Mode Parallel Compound Control for Alternating Current Servo System,” 2012 International Workshop on Information and Electronics Engineering (IWIEE) Procedia Engineering vol. 29, 2055 – 2061, 2012.

[15] Xiujia Chen and Hongdi Qiu, “Research on Single Neuron Adaptive PID Controller applied Mechanics and Materials , Vol. 651-653, pp 826-830, 2014.